Nuclear Instruments and Methods in Physics Research A 608 (2009) 80–85

Contents lists available at ScienceDirect

Nuclear Instruments and Methods in Physics Research A

journal homepage: www.elsevier.com/locate/nima

Study of charge collection efficiency in 4H–SiC Schottky diodes with ^{12}C ions ☆

M. De Napoli [a,b,*], F. Giacoppo [b,c], G. Raciti [a,d], E. Rapisarda [a,d]

[a] Dipartimento di Fisica e Astronomia, Università degli Studi di Catania, Via S. Sofia 64, I-95123 Catania, Italy
[b] Laboratori Nazionali del Sud, Via S. Sofia 62, I-95123 Catania, Italy
[c] Dipartimento di Fisica, Università degli Studi di Messina, Via Salita Sperone 31, I-98166 Messina, Italy
[d] Isituto Nazionale di Fisica Nucleare, Sezione di Catania, Via S. Sofia 64, I-95123 Catania, Italy

ARTICLE INFO

Article history:
Received 21 April 2009
Received in revised form
4 June 2009
Accepted 8 June 2009
Available online 17 June 2009

Keywords:
SiC—silicon carbide
Semiconductors
Radiation detectors

ABSTRACT

The Charge Collection Efficiency (CCE) in 4H–SiC epitaxial Schottky diodes is studied as a function of the applied reverse bias. Three SiC types, with different doping concentrations, were used to detect ^{12}C ions at 14.2, 28.1 and 37.6 MeV. In two SiC types we observe minority charge carriers, generated by the incoming ion in the neutral region, which diffuse to the depleted layer and are finally collected. The minority carriers contribution to the CCE is well reproduced by an analytical equation which represents the contribution from the charge carriers diffusing to the depletion region from the semiconductor substrate. From a best fit procedure, the minority carriers diffusion length is extracted and the minority carriers lifetime is calculated. Finally, the dependence of the lifetime on the doping concentration is investigated.

1. Introduction

Silicon carbide (SiC) is one of the most attractive semiconductor materials as its wide bandgap, high breakdown electric field strength, high saturated drift velocity and large thermal conductivity are promising for high-temperature and high-radiation operating conditions [1]. Moreover, SiC diodes are predicted to be radiation hard with respect to silicon and therefore potentially useful as radiation detectors in very severe environments. A lot of effort has gone into producing good-quality and low-defect SiC diodes based on Schottky diode and p–n junction designs [2–4]. They have already been used to detect neutrons [5], X-rays [6], protons [7], alpha particles [8–10] and heavier ions [11,12]. A review of SiC properties as radiation detector material is reported in Ref. [13]. Recently, in order to explore possible applications in nuclear physics, we have extended the study of SiC detection properties and radiation damage to light ions, ^{12}C and ^{16}O, at energies between 5 and 37.6 MeV [14,15]. In Ref. [15] we found a strong dependence of the energy resolution on the applied reverse bias. This effect, already observed in Refs. [16–18], could be due to the diffusion to the active region of minority charge carriers, produced in the unpolarized part of the detector [17].

In order to investigate on minority carriers diffusion, we studied the Charge Collection Efficiency (CCE) of 4H–SiC Schottky diodes, using them to detect ^{12}C ions at 14.2, 28.1 and 37.6 MeV, as a function of the applied reverse bias. The CCE of 4H–SiC Schottky diodes [17–22] and 6H–SiC p–n junctions [10] have been extensively studied only for protons and alpha particles. The experimental data show, especially at low bias values, an important contribution to the CCE owing to minority carriers diffusion [10,17–22]. This contribution is well reproduced by the diffusion formula proposed by Breese [23] as well as the drift-diffusion simulation program DESSIS [19,21]. In case of heavier ions, the Breese equation was successfully used in 6H–SiC n^+pp^+ diodes irradiated with ^{16}O at 15 MeV [24], but was unable to describe the CCE in 6H–SiC p^+n diodes irradiated with ^{16}O at 9 MeV [25]. The authors suggest, as a possible explanation, the Auger recombination effect [26] due to the elevate carrier injection of a heavy-ion. Therefore, the study of CCE in 4H–SiC using ^{12}C ions extends the existing results, which seem to depend on the diode properties as well as the detected particles.

2. Experimental setup

Three types of SiC Schottky diodes, with different nominal n^- epitaxial layer concentrations and thicknesses, have been used. Their characteristics are reported in Table 1.

☆ Partly supported by the European Community in the framework of the "DIRAC secondary-beams" project, Contract no. 515873 under the "Structuring the European Research Area" Specific Programme Research Infrastructures Action.

* Corresponding author at: Dipartimento di Fisica e Astronomia, Università degli Studi di Catania, Via S. Sofia 64, I-95123 Catania, Italy. Tel.: +39 095 542 305; fax: +39 095 378 5225.
E-mail address: denapoli@lns.infn.it (M. De Napoli).

0168-9002/$ - see front matter © 2009 Elsevier B.V. All rights reserved.
doi:10.1016/j.nima.2009.06.018

Table 1
Characteristics of the three types of tested SiC diodes.

Type	Nominal dopant concentration (N/cm^3)	Thickness (μm)
a	7.6×10^{14}	37.9
b	2.0×10^{15}	43.7
c	1.5×10^{16}	21

The active area of each chip is $2 \times 2\,mm^2$ and the dopant nitrogen concentration and thickness of the n^+ side are $7 \times 10^{18}\,N/cm^3$ and 279 μm, respectively. The diodes have been fabricated by epitaxy onto high-purity 4H–SiC n-type substrate from the ETC-Catania [27]. The Schottky junction was realized by a 0.2 μm thick layer of Ni_2Si deposited at 600 °C on the front surface, while the ohmic contact, on the back surface, was obtained with Ni_2Si deposited at 950 °C [28,29]. The chips were glued onto a brass foil 1 mm thick by conductive glue and single contacts between the Ni_2Si front surfaces and individual pads of a board were realized by Al wire (2 μm thick) bonding. The boards were set up in a scattering chamber at the Laboratori Nazionali del Sud (LNS, Catania) and operated under vacuum at 10^{-6} mbar. Another board was equipped with a Si detector 300 μm thick and $3 \times 3\,cm^2$ of surface which was used as reference. The ^{12}C ion beams, accelerated by the LNS Tandem VdG [30], were focused 60 cm downstream with respect to the detector position in order to achieve a uniform perpendicular irradiation in a spot of about 3 mm of diameter on the SiC surface. Such spot dimension results from the optimization of the beam focusing onto the board holder. Even though the beam spot was larger than the diodes active area, the CCE saturation value of 100%, as explained in the next paragraph, shows that the whole charge produced in the detectors by most of the incoming ions is collected, and therefore charge loss due to edge effects is not observed. The beam spot dimension as well as its stability was monitored by means of an alumina layer, with a hole of 3 mm of diameter, set up on the boards holder and a camera monitoring it. Since the spot position moves with the beam energy, the beam was focused onto the boards holder for each energy change. Once the beam was focused and its spot stability was verified, the boards holder was moved so as to centerthe detectors one by one onto the ion beam.

Standard electronics were used to process the signals: preamplifiers of 45 mV/MeV gain (ORTEC 142A) and amplifiers with 0.5 μs shaping time. Data acquisition was based on CAMAC ADCs read out through a GPIB (General Purpose Interface Bus) standard National Instruments interface and a data-acquisition program built in the LabView 7 framework.

3. Charge collection efficiency

The three types of SiC diodes were used to detect ^{12}C ions at 13.7, 27.7 and 37.3 MeV. These incident energies correspond to 14.2, 28.1 and 37.6 MeV, respectively, once the energy loss in the Ni_2Si 0.2 μm thick front layer, computed by using the SRIM code [31], is taken into account. For each incident energy, a number of energy spectra were taken over a range of reverse bias voltages from 0 to −1000 V. As one can see from Fig. 1, the peak position, evaluated by Gaussian fits of the energy spectra, moves toward higher values as the voltage increases. This effect is due to the increasing thickness of the depleted layer by increasing reverse bias voltage [14,15]. As a result, the incident ^{12}C releases more energy in the active region leading to detector signals with higher pulse-height. The saturation of the peak position is reached when the depleted thickness is larger than the ions range. In this bias region, as we have already observed in Ref. [14], the comparison between the SiC pulse-heights and those obtained from silicon detector shows that the whole charge produced by the incoming ion is collected.

The CCE is defined as the ratio between the collected charge and the charge produced by the particle in the detector. The amount of the collected charge is proportional to the peak position. In particular, since in the signal saturation region all the produced charge is collected, the total charge produced by ^{12}C in the SiC diode is proportional to the saturated peak position. The experimental CCE is therefore extracted as the ratio between the peak position, measured at different applied bias, and its saturation value [32]. Fig. 2 (full squares) shows the experimental CCE for a SiC type b, for the three ^{12}C incident energies. In the same figure the data are compared with theoretical values (full curves) evaluated as

$$CCE_{drift} = \frac{1}{E_0}\int_0^d \frac{dE}{dx}\,dx \tag{1}$$

where E_0 is the total incident energy, d is the thickness of the depleted region and dE/dx is the ion energy loss per unit path length [10,17–20,22]. This equation represents the charge collected from the depletion region where fast charge carriers drift under the influence of the electric field. In the calculations, SRIM dE/dx equations and the corrected ^{12}C incident energies were used. Moreover, the thickness of the depleted region (d), for each applied bias (V), was calculated by using the equation [15]

$$d \approx \sqrt{\frac{2(V + V_{built\text{-}in})\varepsilon}{eN}} \tag{2}$$

where ε and e are the static permittivity of the material and the electron charge, respectively, $V_{built\text{-}in} = 1.5\,V$ [15] is the magnitude of the Schottky barrier height and N is the SiC doping concentration.

As one can clearly see from Fig. 2, in the bias region where the CCE is not saturated, the calculations underestimate the experimental data, at all the incident energies. This result indicates that, in this bias region, more charge than the ionization charge produced by the ions in the depleted layer is collected. As suggested in Refs. [10,17–22,24], the extra collected charge could be due to the minority carriers, generated by the incoming ion in the neutral region, which diffuse to the depleted layer and are finally collected. In order to assess the contribution of minority carrier diffusion, we use the analytical expression proposed by Breese [23]

$$CCE_{diffusion} = \frac{1}{E_0}\int_d^D \frac{dE}{dx} e^{-x-d/L_p}\,dx \tag{3}$$

where D is the thickness of the active layer and L_p is the minority carrier diffusion length, i.e. the average distance that a minority carrier diffuses before it recombines with a majority carrier. The $CCE_{diffusion}$ calculations, shown in Fig. 2 as dashed curves, well reproduce the differences between the experimental CCE and the CCE_{drift} (empty squares) at all the incident energies. In particular, the minority carrier diffusion length L_p, extracted from a best fit procedure, is 7 ± 1 μm. This value generally depends on the type and the concentration of impurities in the crystal, the number of defects and these energy states. However, it is on the same order of magnitude of those reported in Refs. [10,17–22,33]. It must be noted that it is possible to fit the data for the three ^{12}C incident energies with a single value of L_p. We do not observe a worsening of the fit quality as the ion energy decreases, as reported for alpha particles in Ref. [22] and ascribed to plasma effects [34].

The same analysis was also performed on SiC types a and c, and results are shown in Figs. 3 and 4, respectively. In case of SiC type c we did not measure the energy spectra for ^{12}C ions at 37.3 MeV

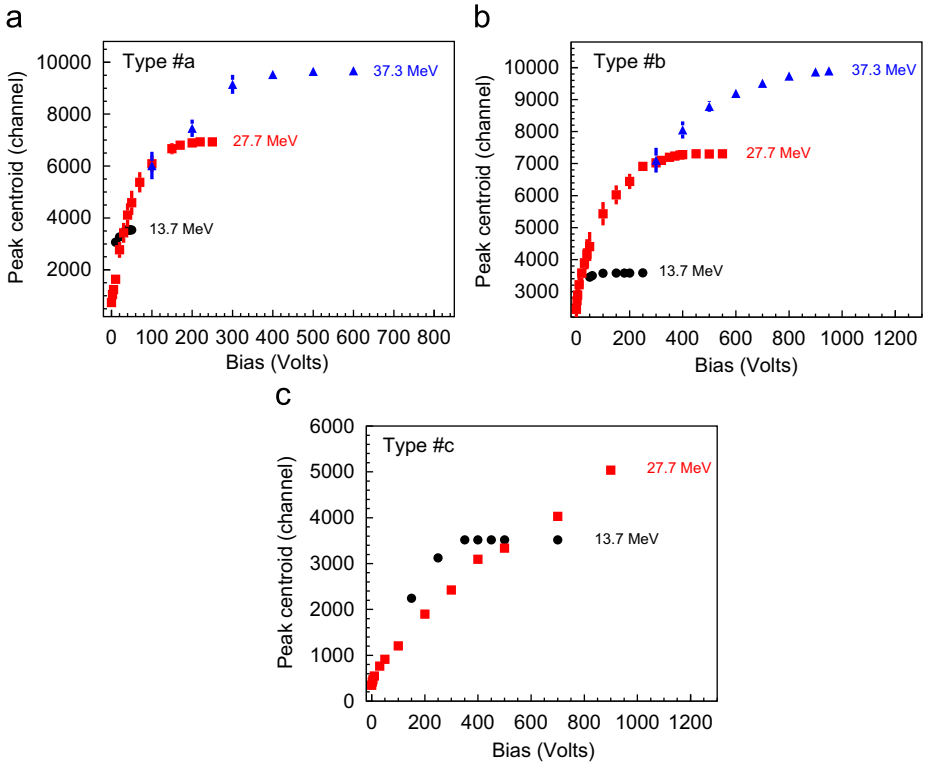

Fig. 1. Centroid value of the energy peak of the ^{12}C at 13.7 (circles), 27.7 (squares) and 37.3 MeV (triangles), as a function of the reverse bias applied to SiC a (top panel), b (middle panel) and c (bottom panel). The figures are taken from Ref. [15].

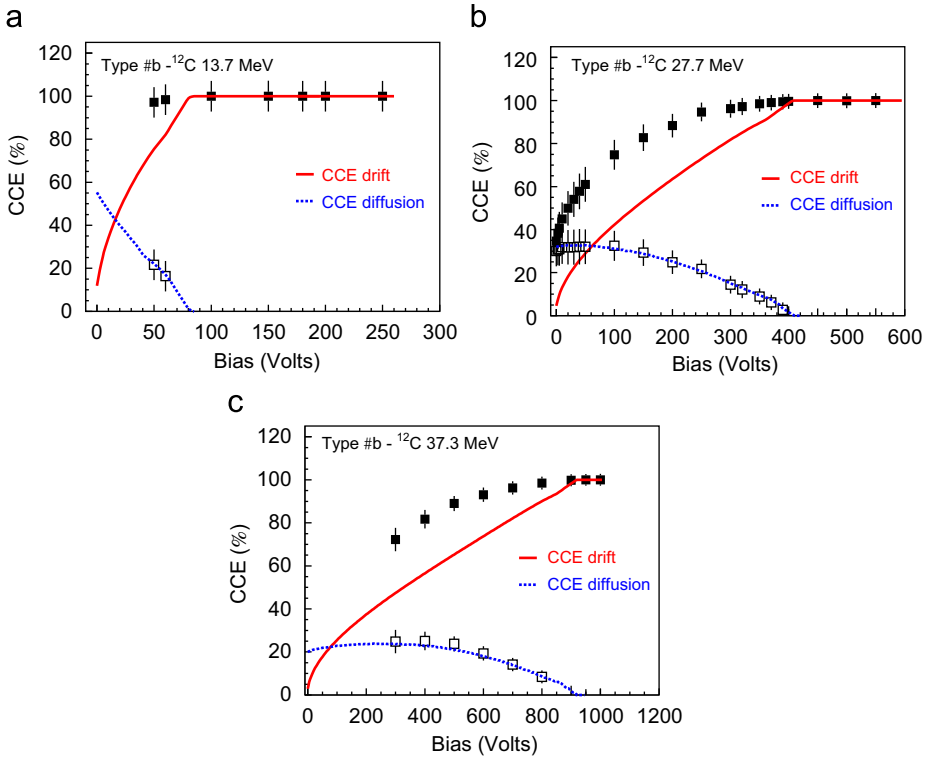

Fig. 2. Experimental CCE of an SiC type b (full squares) as a function of the applied reverse bias for ^{12}C ions at 13.7 (top panel), 27.7 (middle panel) and 37.3 MeV (bottom panel). The full curves represent the theoretical values obtained from Eq. (1). The empty squares are the differences between the experimental points and the theoretical predictions and the dashed curves are the best fits of the empty squares, performed by using Eq. (3).

since, already for ^{12}C ions at 27.7 MeV, the signal-height does not saturate (Fig. 1, bottom panel). In fact the range of ^{12}C at 27.7 MeV can be reached only at voltages higher than the preamplifiers limit [15]. Since no saturation is observed, in case of ^{12}C at 27.7 MeV, the CCE is therefore extracted as the ratio between the position of the calibrated energy spectra and the ^{12}C incident energy.

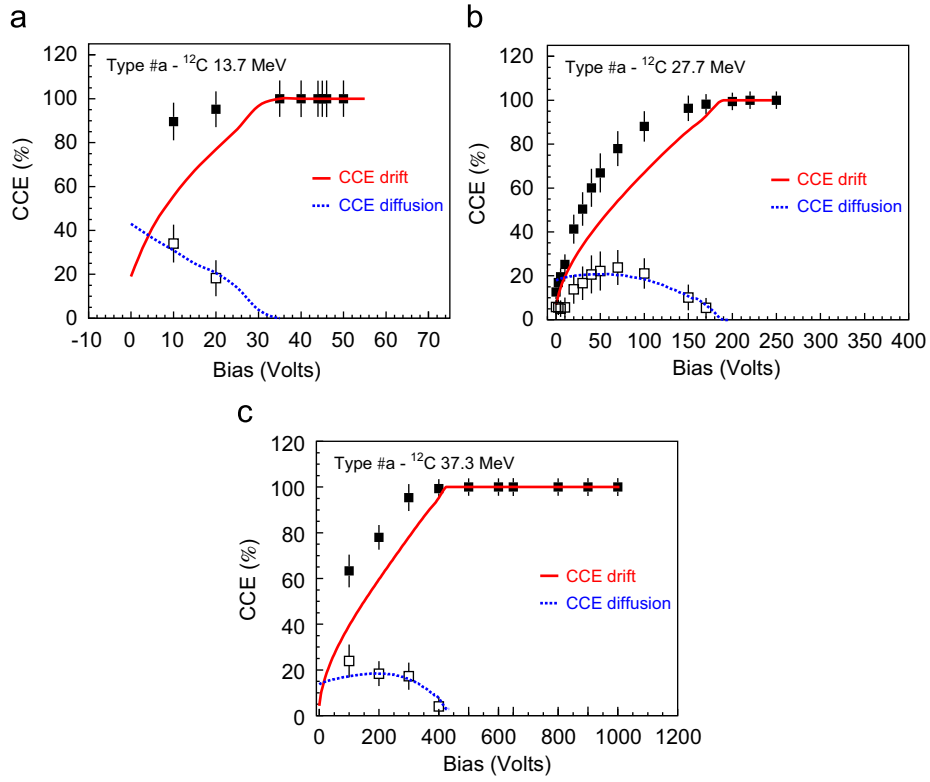

Fig. 3. The same of Fig. 2 for SiC type a.

As one can see from Fig. 3, a contribution to the CCE owing to minority carriers diffusion is also observed in SiC type a for which the extracted L_p value is $5 \pm 1\,\mu m$. On the contrary, as shown in Fig. 4, the CCE in SiC type c is well reproduced by the CCE_{drift} calculations. The peak position is only due to the collection of primary ionization charges, generated by the ion within the depleted region, and no minority carriers diffusion is observed.

The lack of minority carriers collection could be due to an high concentration of defects in the crystal. These defects can act as trapping centers for minority carriers, reducing the probability of their diffusion through the crystal. In fact, as observed in Refs. [18,19,22], the presence of defects reduces the minority carriers diffusion length and lifetime. The time for carriers to diffuse to the edge of the depletion layer can be calculated as $z^2/4D_a$ [23], where z is the distance from the point of creation of the carriers to the depletion region edge and D_a is the ambipolar diffusion coefficient. For 27.7 MeV ^{12}C, which have a range of 19.7 μm in SiC, the time taken can be as long as 800 ns. Since this time can be considerably longer than the carrier lifetime (see next paragraph), trapping and recombination reduce the number of carriers that diffuse to the edge of the depletion region, and so reduces the number of charge carriers measured from the substrate. On the other side, charge carriers created in the semiconductor depletion region are separated under the influence of the electric field and the time they take to cross the depletion region is of the order of ps [23], which is much shorter than the carrier lifetime. Therefore in the depletion region the defects are much more less effective [18,19,22] and, when enough defects are present in the crystal, the CCE can be reproduced by the CCE_{drift} calculations [18,19,22], as in case of SiC type c. An higher concentration of defects in SiC type c than in type a or b could depend on the fact that the diodes are made on different wafers. Moreover, it could be also due to different epitaxial growth conditions and/or to the higher nitrogen doping concentration of SiC type c with respect to types a and b. Indeed, dominant defects in n-type 4H–SiC are the $Z_{1,2}$ centers, a complex of a single nitrogen atom together with an intrinsic center such as carbon interstitial or silicon vacancy [35]. $Z_{1,2}$ have a large capture cross-section for holes and therefore dominate the minority carriers lifetime in n^- epilayers [36]. The concentration of such defects depends on several epitaxial growth parameters such as C/Si ratio, growth temperature, pressure and position of the wafer along the gas flow direction [37,38], and increases by increasing the nitrogen concentration [37].

Finally, in Ref. [15] we have measured the energy resolution of the three SiC types as a function of the applied bias. In the bias region where the depleted layer is smaller than the ions range, we have observed a poorer energy resolution for SiC types a and b than for SiC type c. Moreover, in the same bias region, SiC types a and b have shown a large improvement of the energy resolution by increasing the bias voltage up to the values for which the pulse-height saturation is reached. The results of the present work support the idea that the low energy resolution and its dependence on the applied bias could be due to minority carriers diffusion. In particular, the improvement of the energy resolution by increasing the applied bias, corresponds to the decrease of collected minority carriers, observed in Figs. 2 and 3. Random recombinations of minority carriers and their long collection time could, in fact, generate large fluctuations in the amount of collected charge and ballistic defects [17,39].

4. Minority carriers lifetime

The minority carriers lifetime τ_p is an important property of any semiconductor. It has been calculated, as in Refs. [10,17,19,22], by using the equation

$$L_p = (D_p \tau_p)^{1/2} \tag{4}$$

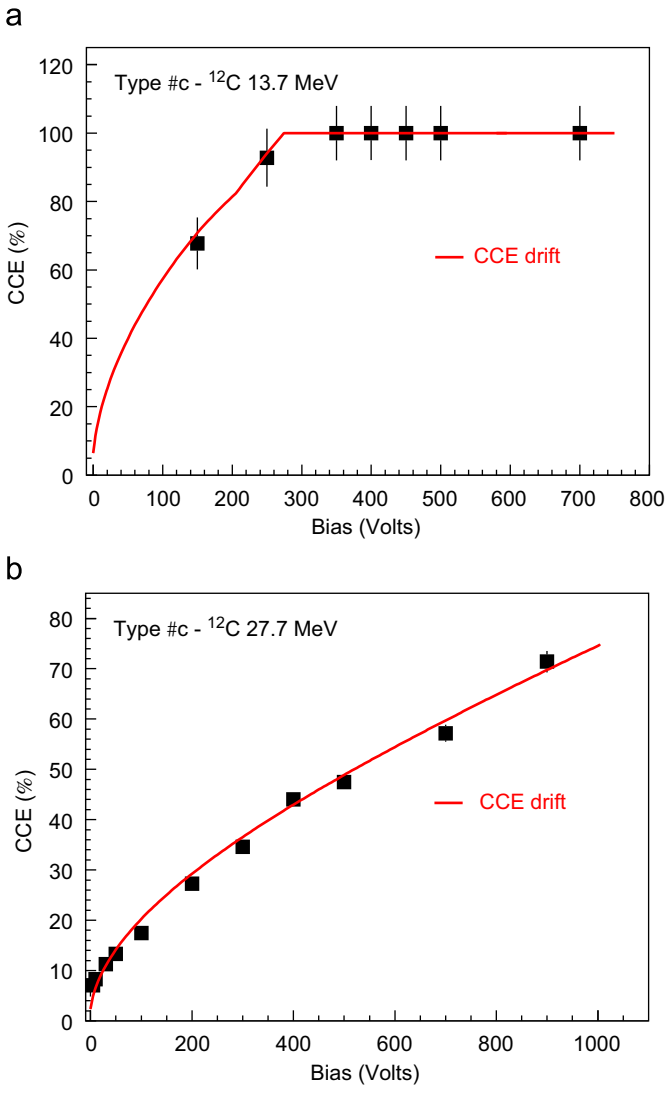

Fig. 4. The same of Fig. 2 for SiC type c.

and the Einstein formula [40]

$$D_p = (kT/e)\mu_p \tag{5}$$

where D_p is the diffusion coefficient, μ_p is the ohmic hole mobility, T is the temperature and e the electron charge. In particular, by using the extracted diffusion lengths, a ohmic hole mobility of $120\,\mathrm{cm^2\,V^{-1}\,s^{-1}}$ [22] and a temperature of 25 °C, the calculated minority carrier lifetimes are 52 ± 20 and 160 ± 40 ns for SiC types a and b, respectively.

Fig. 5 (empty squares) shows the calculated lifetimes as a function of the doping concentration. In the same figure 4H–SiC data from Refs. [7,17,18,20–22,33] and 6H–SiC data from Refs. [10,24] are reported.

The reported data agree quite well for doping concentration values above $10^{15}\,\mathrm{cm^{-3}}$ whereas, for values below $10^{15}\,\mathrm{cm^{-3}}$, large variations are observed. The variations could be due to different types and concentrations of defects in the diodes which are predicted to affect the lifetime, especially at low doping concentrations [41]. However, despite these large variations, the overall trend is a decrease of the lifetime by increasing the doping concentration. This behavior is similar to the one observed in Si [42,43], Ge [44,45], GaP [46] and HgCdTe [47] when averaging data of a wide range of experiments and can be explained by considering the recombination processes which determine the

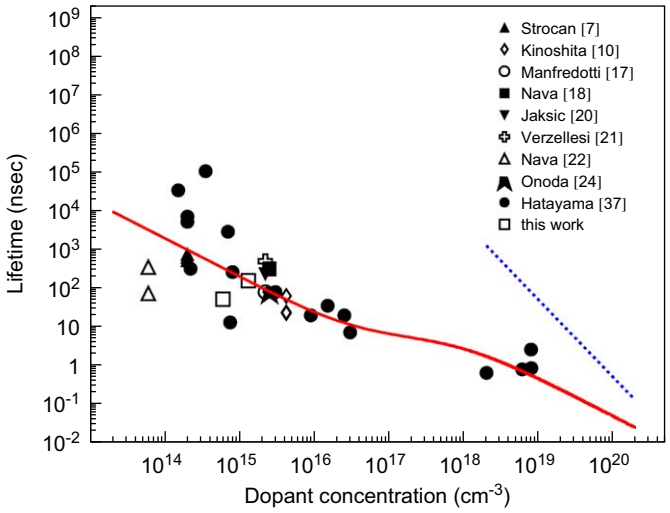

Fig. 5. Minority carriers lifetime as a function of the dopant concentration (error bars are within the size of the symbols). The lifetime values of Refs. [7,20,24,33] are calculated from Eqs. (4) and (5). The full curve shows the lifetime calculated from Eq. (6) and the dashed curve shows the band-to-band Auger lifetime.

carriers lifetime. Generally it depends on the simultaneous action of the Shockley–Read–Hall (SRH) and Auger recombination mechanisms. The SRH recombination results from the thermal recombination of one electron and one hole through defect levels located in the bandgap of the material, whereas the band-to-band Auger recombination is a process in which an electron and a hole recombine in a band-to-band transition, with the resulting energy given off to another electron or hole. The lifetime dependence on doping concentration N can be approximated, as in case of Ge [44,45], by a phenomenological $1/N$ dependence

$$\tau = \frac{\tau_{SRH}}{1 + N/N_{thr}} \tag{6}$$

where N_{thr} is a threshold doping density, which for Ge is assumed to be $N_{thr} = 4 \times 10^{16}\,\mathrm{cm^{-3}}$ [44,45], and τ_{SRH} can be calculated as [45,48]

$$\tau_{SRH} = \frac{1}{n_0 + p_0}[(\sigma_n N_T \nu_{th})^{-1}(p_0 + N_V e^{-(E_T - E_V)/KT}) + (\sigma_p N_T \nu_{th})^{-1}(n_0 + N_C e^{-(E_C - E_T)/KT})] \tag{7}$$

where N_T is the trap density, E_T is the trap energy, σ_n and σ_p are the trap cross-sections for electrons and holes, N_V and N_C are the density of states in the valence and conduction bands, E_V and E_C are the valence and conductive band energies, T is the temperature, n_0 and p_0 are the equilibrium densities of electrons and holes, ν_{th} is the thermal velocity.

The full curve in Fig. 5 represent the lifetime values calculated from Eq. (6) using a threshold doping density of $N_{thr} = 9 \times 10^{17}\,\mathrm{cm^{-3}}$, a shallow trap energy E_T of 0.15 eV and a product of the trap capture cross-section and trap density $\sigma_n N_T = \sigma_p N_T = 15\,\mathrm{cm^{-1}}$. As one can see from Fig. 5, for doping concentrations below $10^{15}\,\mathrm{cm^{-3}}$, the different data cannot be reproduced with a single curve since τ_{SRH}, especially at low doping concentrations, depends on the properties of the lifetime-limiting defects which are often a function of growth technique and device fabrication process. On the contrary, for doping concentrations above $10^{15}\,\mathrm{cm^{-3}}$, the lifetime dependence on doping concentration is, on average, well approximated by Eq. (6).

The observed lifetime decrease, at high doping concentrations, does not seem to directly depend on band-to-band Auger recombinations. In fact the band-to-band Auger lifetime, calculated as $\tau_{Auger} = 1/(CN^2)$ with $C = 2 \times 10^{-31}\,\mathrm{cm^6 s^{-1}}$ [49] (dashed

line of Fig. 5), overestimates the experimental data. Therefore, a possible explanation of the observed $1/N$ dependence could be the presence of dopant-related traps and trap-assisted Auger processes [44], summarized by the N_{thr} parameter. Indeed, it has been shown by several authors that trap levels in Si due to dopants, impurities or defect can introduce trap-assisted Auger recombinations [50–52].

5. Conclusions

In the present work the CCE of 4H–SiC Shottky diodes has been investigated as a function of the applied reverse bias. Three types of SiC diodes, with different doping concentrations, were used to detect ^{12}C ions at 14.2, 28.1 and 37.6 MeV. For the three SiC types, the experimental CCE increases by increasing the reverse bias, since the diode active layer widens and more energy is deposited within the depleted thickness. When the whole ^{12}C incident energy is deposited within the depleted thickness the CCE saturates. The share of charge collected from the depletion region is calculated by means of the CCE_{drift} equation (Eq. (1)). The calculations well reproduce the data of SiC type c but underestimate, at all the incident energies, those of SiC types a and b. This result could be explained by the collection of minority carriers which are generated by the incoming ion in the neutral region and diffuse toward the active layer.

The $CCE_{diffusion}$ equation (Eq. (3)), proposed by Breese [23] in order to assess the contribution to the CCE owing to minority carrier diffusion, well reproduces the differences between the experimental CCE and the CCE_{drift} calculations. This result shows that the Breese equation, which in 4H–SiC diodes has been extensively used only for protons and alpha particles [10,17–20,22], is also able to reproduce the contribution of minority carriers diffusion to the CCE in 4H–SiC when heavier ions are detected.

Finally, the doping dependence of the minority carriers lifetime has been investigated. Despite some large differences between the reported data, a decrease of the lifetime by increasing the doping concentration is observed. In particular, the dependence of lifetime on doping concentration can be approximated by a phenomenological $1/N$ dependence which could reflect the presence of dopant-related traps and trap-assisted Auger processes.

Acknowledgments

Help in the SiC diodes selection and wire bonding realization as well as the valuable discussion with L. Calcagno, G. Foti and F. La Via are greatly appreciated. M.D. and E.R. acknowledge the support from the European Community in the framework of the "DIRAC secondary-beams"—Contract no. 515873 under the "Structuring the European Research Area" Specific Programme Research Infrastructures Action.

References

[1] G.L. Harris (Ed.), Properties of Silicon Carbide, EMIS Datareviews Series no. 13, an INSPEC Publication, Institution of Electrical Engineering, London, UK, 1995.
[2] F.H. Ruddy, A.R. Dulloo, J.G. Seidel, S. Seshadri, L.B. Rwland, IEEE Trans. Nucl. Sci. NS-45 (1998) 536.
[3] M. Rogalla, K. Runge, A. Soldner-Rembold, Nucl. Phys. B 78 (Proc. Suppl.) (1999) 516.
[4] M. Bruzzi, F. Nava, S. Russo, S. Sciortino, P. Vanni, Diamond Relat. Mater. 10 (2001) 657.
[5] A.R. Dulloo, F.H. Ruddy, J.G. Seidel, J.M. Adams, J.S. Nico, D.M. Gilliam, Nucl. Instr. and Meth. A 422 (1999) 47.
[6] G. Bertuccio, R. Casiraghi, A. Cetronio, C. Lanzieri, F. Nava, Nucl. Instr. and Meth. A 522 (2004) 413.
[7] N.B. Strokan, A.M. Ivanov, A.A. Lebev, Nucl. Instr. and Meth. A 569 (2006) 758.
[8] F. Nava, P. Vanni, C. Lanzieri, C. Canali, Nucl. Instr. and Meth. A 437 (1999) 354.
[9] F.H. Ruddy, A.R. Dulloo, J.G. Seidel, J.W. Palmour, R. Singh, Nucl. Instr. and Meth. A 505 (2003) 159.
[10] A. Kinoshita, M. Iwami, K. Kobayashi, I. Nakano, R. Tanaka, T. Kamiya, A. Ohi, T. Ohshima, Y. Fukushima, Nucl. Instr. and Meth. A 541 (2005) 213.
[11] K.K. Lee, T. Ohshima, A. Saint, T. Kamiya, D.N. Jamieson, H. Itoh, Nucl. Instr. and Meth. B 210 (2003) 489.
[12] C. Kamezawa, H. Sindou, T. Hirao, H. Ohyama, S. Kuboyama, Physica B 376–377 (2006) 362.
[13] F. Nava, G. Bertuccio, A. Cavallini, E. Vittone, Meas. Sci. Technol. 19 (2008) 102001.
[14] M. De Napoli, G. Raciti, E. Rapisarda, C. Sfienti, Nucl. Instr. and Meth. A 572 (2007) 831.
[15] M. De Napoli, F. Giacoppo, G. Raciti, E. Rapisarda, Nucl. Instr. and Meth. A 600 (2009) 618.
[16] A.M. Ivanov, N.B. Strokan, D.V. Davydov, N.S. Savkina, A.A. Lebedev, Yu. T. Mironov, G.A. Riabov, E.M. Ivanov, Appl. Surf. Sci. 184 (2001) 431.
[17] C. Manfredotti, F. Fizzotti, A. Lo Giudicie, C. Paolini, E. Vittone, F. Nava, Appl. Surf. Sci. 184 (2001) 448.
[18] F. Nava, E. Vittone, P. Vanni, P.G. Fuochi, C. Lanzieri, Nucl. Instr. and Meth. A 514 (2003) 126.
[19] F. Nava, E. Vittone, P. Vanni, G. Verzellesi, P.G. Fuochi, C. Lanzieri, M. Glaser, Nucl. Instr. and Meth. A 505 (2003) 645.
[20] M. Jaksic, Z. Bosnjak, D. Gracin, Z. Medunic, Z. Pastuovic, E. Vittone, F. Nava, Nucl. Instr. and Meth. B 188 (2002) 130.
[21] G. Verzellesi, P. Vanni, F. Nava, C. Canali, Nucl. Instr. and Meth. A 476 (2002) 717.
[22] F. Nava, G. Wagner, C. Lanzieri, P. Vanni, E. Vittone, Nucl. Instr. and Meth. A 510 (2003) 273.
[23] M.B.H. Breese, J. Appl. Phys. 74 (1993) 3789.
[24] S. Onoda, T. Ohshima, T. Hirao, K. Mishima, S. Hishiki, N. Iwamoto, K. Kojima, K. Kawano, IEEE Trans. Nucl. Sci. NS-54 (6) (2007) 1953.
[25] S. Onoda, T. Ohshima, T. Hirao, K. Mishima, S. Hishiki, N. Iwamoto, K. Kawano, IEEE Trans. Nucl. Sci. NS-54 (6) (2007) 2706.
[26] L.D. Edmonds, IEEE Trans. Nucl. Sci. NS-38 (6) (1991) 1935.
[27] E.T.C. Epitaxial Tecnology Center 207, Corso Italia, I-95127 Catania, Italy.
[28] F. La Via, F. Roccaforte, A. Maktari, V. Raineri, P. Musumeci, L. Calcagno, Microelectron. Eng. 60 (2002) 269.
[29] F. Roccaforte, F. La Via, V. Raineri, P. Musumeci, L. Calcagno, Appl. Phys. A 88 (2003) 827.
[30] G. Ciavola, L. Calabretta, G. Cuttone, S. Gammino, G. Raia, D. Rifuggiato, A. Rovelli, V. Scuderi, Nucl. Instr. and Meth. A 328 (1993) 64.
[31] J.F. Ziegler, J.P. Biersack, IBM-research, Yorktown Heights, New York, USA, 1996.
[32] L. Berluti, C. Canali, A. Castaldini, A. Cavallini, A. Cetronio, S. D'Auria, C. del Papa, C. Lanzieri, G. Mattei, F. Nava, M. Proia, P. Rinaldi, A. Zichichi, Nucl. Instr. and Meth. A 354 (1995) 364.
[33] T. Hatayama, H. Yano, Y. Uraoka, T. Fuyuki, Microelectron. Eng. 83 (2006) 30.
[34] E. Vittone, F. Fizzoni, A.L. Giudice, C. Paolini, C. Manfredotti, Nucl. Instr. and Meth. B 161 (2000) 446.
[35] T.A.G. Eberlein, R. Jones, P.R. Briddon, Phys. Rev. Lett. 90 (2003) 225502-1.
[36] P.B. Klein, B.V. Shanabrook, S.W. Huh, A.Y. Polyakov, M. Skowronski, J.J. Sumakeris, M.J. O'Loughlin, Appl. Phys. Lett. 88 (2006) 052110.
[37] I. Pintilie, L. Pintilie, K. Irmscher, B. Thomas, Appl. Phys. Lett. 81 (2002) 4841.
[38] J. Zhang, L. Storasta, J.P. Bergman, N.T. Son, E. Jazen, J. Appl. Phys. 93 (2003) 4708.
[39] F.S. Goulding, D.A. Landis, IEEE Trans. Nucl. Sci. NS-35 (1988) 119.
[40] S.M. Sze, Physics of Semiconductor Devices, second ed., Wiley, New York, 1981.
[41] J.S. Blakemore, Semiconductor Statistics, Pergamon Press, Oxford, 1962.
[42] E. Mark, E. Solley, M. Liang, D.E. Burk, IEEE Electron Device Lett. 12 (1991) 401.
[43] J.G. Fossum, D.S. Lee, Solid-State Electron. 25 (1982) 741.
[44] E. Gaubas, J. Vanhellemont, Appl. Phys. Lett. 89 (2006) 142106.
[45] E. Gaubas, J. Vanhellemont, E. Simoen, I. Romandic, W. Geens, P. Clauws, Physica B 401 (2007) 222.
[46] M.L. Young, D.R. Wight, J. Phys. D Appl. Phys. 7 (1974) 1824.
[47] M.A. Kinch, F. Aqariden, D. Chandra, P.-K. Liao, H.F. Schaake, H.D. Shih, J. Electron. Mater. 34 (2005) 880.
[48] S.A. Ringel, A. Rohatgi, IEEE Trans. Electron Devices ED-38 (1991) 2402.
[49] ⟨http://www.ioffe.rssi.ru/SVA/NSM/Semicond/SiC⟩.
[50] A. Haug, Phys. Status Solidi B 108 (1981) 443.
[51] M.V. Strikha, Sov. Phys. Semicond. 15 (1985) 429.
[52] P.T. Landsberg, Appl. Phys. Lett. 50 (1987) 745.